

Spin triangle chain with ferromagnetic and antiferromagnetic interactions on the transition line

V. Ya. Krivnov* and D. V. Dmitriev
*Institute of Biochemical Physics of RAS,
Kosygin str. 4, 119334, Moscow, Russia.*

(Dated:)

We investigate spin- $\frac{1}{2}$ anisotropic model of a linear chain of triangles with competing ferro- and antiferromagnetic interactions and ferromagnetic Heisenberg interactions between triangles. For a certain ratio between interactions the one-magnon excitation band is dispersionless leading to an existence of localized-magnon states which form macroscopically degenerated ground states. The spectrum of excitations has a specific structure depending on the value of the triangle-triangle interaction. Such specific structure determines the low-temperature thermodynamics and, in particular, the temperature dependence of a specific heat. In the limit of strong anisotropy of interactions the spectrum has a multi-scale structure which consists of subsets rank-ordered on small parameter. Each subset is responsible for the appearance of the peak in the temperature dependence of the specific heat.

I. INTRODUCTION

Low-dimensional quantum magnets on geometrically frustrated lattice have been extensively studied [1, 2]. An important class of these systems includes lattice consisting of triangles. For special relations between exchange interactions such systems have a dispersionless one-magnon band (flat-band). There is a wide class of the frustrated quantum antiferromagnets (AF) in which a flat-band exists [3–8]. The one-magnon flat-band leads to an existence of localized multi-magnon states which form a macroscopically degenerate ground state in the saturation magnetic field. Such models have specific low-temperature properties such as an jump in the magnetization curve, an extra low-temperature peak in

*Electronic address: krivnov@deom.chph.ras.ru

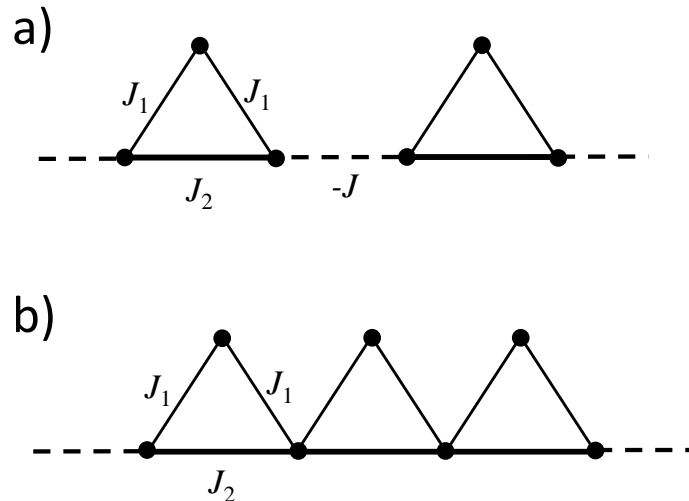


FIG. 1: (a) Model of linear chain of connected triangles and (b) \triangle -chain model.

the specific heat, nonzero residual entropy, etc. [7–13].

An interesting one-dimensional example of such systems is spin- $\frac{1}{2}$ delta-chain consisting of a linear chain of connected triangles as shown in Fig.1. The ground state and the low-temperature properties of the AF delta-chain with flat-band have been studied in detail [5–7, 11, 14–16] and it was shown that it exhibits a number of peculiar properties.

Another class of the frustrated quantum systems with exact localized multi-magnon states are the models with competing ferro- and antiferromagnetic interactions (F-AF models). At definite value of the ratio of these interactions the model has massively degenerate ground state at zero magnetic field. The main difference between AF and F-AF models with flat-band consists of additional specifically overlapping localized multi-magnon complexes which are exact ground states together with isolated localized magnons. It leads to the macroscopical degeneracy of the ground state and the residual entropy is larger than that for the AF models. The example of this model is the same delta-chain. The properties of the F-AF delta-chain has been studied in [17–21]. In these works the ground state degeneracy has been determined and the relation of the low-energy excitations to the low-temperature properties has been studied.

In this paper we study another example of the frustrated spin- $\frac{1}{2}$ model with ferromagnetic and antiferromagnetic interactions. This model represents a linear chain of triangles connected by the ferromagnetic Heisenberg interactions (spin- $\frac{1}{2}$ triangle chain model) as

shown in Fig.1. The interaction J_1 between the basal and the apical spins of triangle is ferromagnetic and the basal-basal interaction J_2 is antiferromagnetic. The interaction J between triangles is ferromagnetic. The Hamiltonian of this model has a form

$$H = \sum_{i=1}^n H_i + \sum_{i=1}^n V_{i,i+1} \quad (1)$$

where

$$\begin{aligned} H_i &= J_1 \sum_{m=1,2} \left(s_{i,m}^x s_{i,m+1}^x + s_{i,m}^y s_{i,m+1}^y + \Delta_1 (s_{i,m}^z s_{i,m+1}^z - \frac{1}{4}) \right) \\ &\quad + J_2 \left(s_{i,1}^x s_{i,3}^x + s_{i,1}^y s_{i,3}^y + \Delta_2 (s_{i,1}^z s_{i,3}^z - \frac{1}{4}) \right) \\ V_{i,i+1} &= -J (\mathbf{s}_{i,3} \mathbf{s}_{i+1,1} - \frac{1}{4}) \end{aligned} \quad (2)$$

where n is a number of triangles, Δ_1 and Δ_2 are parameters of the anisotropy of the basal-apical and the basal-basal interactions ($\Delta_1, \Delta_2 > 0$). The constants in Eq.(2) are chosen so that the energy of the ferromagnetic state with $S^z = \pm \frac{3}{2}n$ is zero. The periodic boundary conditions are imposed. Further we put $J_1 = -1$ and $J_2 = \alpha$.

Model (1) is an extension of the F-AF delta chain. We will show that the spin- $\frac{1}{2}$ triangle model (1) has a huge manifold of ground states and we focus on the studies of the influence of the triangle-triangle ferromagnetic interactions on the ground state properties and on the low-temperature thermodynamics.

The paper is organized as follows. In Sec.II we derive the necessary conditions on the Hamiltonian parameters for which the model has exact localized magnon states. In Sec.III we study the spin triangle model on the transition line between different phases and represent the results for the ground state degeneracy. Here we also study the structure of the spectrum and the density of states and their relation to the low-temperature thermodynamics. In Sec.IV we study the properties of the model with strong anisotropy of interactions. In Sec.V we give a summary of our results.

II. FLAT-BAND AND LOCALIZED MAGNONS

At first, we calculate the energy of one-magnon states, i.e. the states in the spin sector $S^z = S_{\max} - 1$ ($S_{\max} = \frac{3}{2}n$). The one-magnon energy $E(k)$ can be found from the equation

$$(E(k) - \Delta_1) [(E(k) + A)^2 - (E(k) + A)(\alpha + J) + \frac{\alpha J}{2}(1 + \cos k)] - \frac{E(k) + A}{2} + \frac{J}{4}(1 + \cos k) = 0 \quad (3)$$

where $A = \frac{1}{2}(\Delta_1 - \alpha(1 + \Delta_2))$.

There are three branches of the one-magnon energy and the lowest branch $E_1(k)$ becomes dispersionless (flat band) under the condition

$$\Delta_2 = \frac{1}{\alpha^2} - \frac{\Delta_1}{\alpha} - 1 \quad (4)$$

and $E_1(k)$ is

$$E_1(k) = \Delta_1 - \frac{1}{2\alpha} \quad (5)$$

We notice that the condition (4) and the energy E_1 do not depend on J .

The energy of two other branches are

$$E_{2,3}(k) = E_1 + \frac{1}{2} \left[\alpha + J + \frac{1}{2\alpha} \pm \sqrt{(\alpha - J + \frac{1}{2\alpha})^2 + 2\alpha J(1 - \cos k)} \right] \quad (6)$$

and $E_{2,3}(k) > E_1$.

The one-magnon flat band means the existence of the localized states which can be chosen as

$$\varphi_{m,m+1} |F\rangle = (s_{m,2}^- + \alpha s_{m,3}^- + \alpha s_{m+1,1}^- + s_{m+1,2}^-) |F\rangle \quad m = 1, 2, \dots, n \quad (7)$$

where $|F\rangle$ is the ferromagnetic state with all spins up and s_i^- is the spin lowering operator.

The wave function (7) is localized in the valley between neighboring triangles. Because one magnon is localized between m and $(m+1)$ triangles it is possible to construct $k \leq n/2$ non-overlapping localized (independent) magnons with the total energy $E_k = kE_1$ and all of them are exact states. If $E_1 < 0$ ($\Delta_1 < \frac{1}{2\alpha}$) the lowest energy of these states is realized in the spin sector $S^z = S_{\max} - n/2$. The numerical calculations show that at $\Delta_1 < \frac{1}{2\alpha}$ the ground state of model (1) is in the spin sector $S^z = 0$. For $E_1 > 0$ the ground state is ferromagnetic with zero energy.

III. SPIN TRIANGLE CHAIN ON THE TRANSITION LINE

The ferromagnetic state for model (1) becomes unstable when one-magnon excitations becomes negative. Therefore, the transition line between the ferromagnetic and other (ferromagnetic or $S^z = 0$) ground state phases is defined by the condition $E_1 = 0$. In this case the model is described by one parameter that is convenient to choose as Δ_1 , and according to conditions (4), (5) two other parameters are $\alpha = \frac{1}{2\Delta_1}$ and $\Delta_2 = 2\Delta_1^2 - 1$. The model on the

transition line has the macroscopically degenerated ground state. To explain this fact let us consider one separate triangle H_i . From eight eigenstates of H_i six states has zero energy: two states with $S^z = \pm 3/2$ and four states with $S^z = \pm 1/2$. The energy of two other states with $S^z = \pm 1/2$ is positive and it is $E = \Delta_1 + \frac{1}{2\Delta_1}$. Because the Hamiltonians H_i and $V_{i,i+1}$ do not commute with each other the ground state energy E_0 of H satisfies an inequality

$$E_0 \geq E_0(i) + E_0(i, i+1) = 0 \quad (8)$$

where $E_0(i)$ and $E_0(i, i+1)$ are the ground state energies of H_i and $V_{i,i+1}$ which are zero. Since independent magnon states have zero energy, the inequality (8) becomes the equality and all such states are ground states. In Refs.[17, 18, 21] it was shown that in the F-AF delta-chain in addition to isolated magnon states there are overlapping magnon states of a special form which are exact ground states as well. As follows from Eq.(4) the conditions for the existence of exact magnon states do not depend on the triangle-triangle interaction J (if $J > 0$) and the ground state manifold of model (1) on the transition line is similar to that for the F-AF delta-chain. We note that at $J = 0$ the ground state is 6^n -degenerated and the triangle-triangle interaction J lifts this degeneracy but a part of 6^n states remains degenerated with zero energy. The number of such ground states in each spin sector can be obtained using the results of Refs.[17, 18, 21] taking into account minor corrections. We will not give details of these calculations and present the final results only.

For the model with open boundary condition (OBC) for any value of Δ_1 the number of the ground state $W_k(n)$ in the spin sectors $S^z = S_{\max} - k$ and $S^z = -S_{\max} + k$ is

$$\begin{aligned} W_k(n) &= \sum_{m=0}^k C_n^m, & 0 \leq k \leq n \\ W_k(n) &= 2^n, & n < k \leq \frac{3n}{2} \end{aligned} \quad (9)$$

where $C_n^m = n!/m!(n-m)!$ are binomial coefficients.

The total number of the ground states $G(n)$ is

$$G(n) = \sum_k W_k(n) = (2n+1)2^n \quad (10)$$

The number of the ground states for the model with periodic boundary conditions (PBC) is given by

$$\begin{aligned} W_k(n) &= C_n^k, & 0 \leq k \leq \frac{n}{2} \\ W_k(n) &= C_n^{n/2}, & \frac{n}{2} < k \leq \frac{3n}{2} \end{aligned} \quad (11)$$

The total number of the ground states is

$$G(n) = 2^n + 2nC_n^{m/2} \quad (12)$$

Eq.(11) is valid for all $0 < \Delta_1 < \infty$ except two special cases, $\Delta_1 = \frac{1}{\sqrt{2}}$ and $\Delta_1 = \frac{1}{2}$. For the model with $\Delta_1 = \frac{1}{\sqrt{2}}$ the number $W_k(n)$ is

$$\begin{aligned} W_k(n) &= C_n^0 + C_n^2 + \dots + C_n^k, & \text{even } k \leq n \\ W_k(n) &= C_n^1 + C_n^3 + \dots + C_n^k, & \text{odd } k \leq n - 1 \\ W_k(n) &= 2^{n-1}, & n < k \leq \frac{3n}{2} \end{aligned} \quad (13)$$

The total number of the ground state for this special case is

$$G(n) = 2^n(n + 1) \quad (14)$$

The number of the ground state for the case $\Delta_1 = \frac{1}{2}$ is

$$W_k(n) = C_n^k + b_{n,k} \quad (15)$$

where

$$\begin{aligned} b_{n,k} &= C_n^{k-3}, & 3 \leq k \leq \frac{n}{2} \\ b_{n,k} &= 2C_n^{m/2-3} - C_n^{m-k-3}, & \frac{n}{2} + 1 \leq k \leq n - 3 \\ b_{n,k} &= 2C_n^{m/2-3}, & n - 2 \leq k \leq \frac{3n}{2} \end{aligned} \quad (16)$$

The total number of the ground states in this case is

$$G(n) = 2^n + 2nC_n^{m/2} + 6(n - 2)C_n^{m/2-3} \quad (17)$$

We note that the ground state degeneracies $W_k(n)$ and $G(n)$ on the transition line do not depend on J including the case $J \rightarrow \infty$, when spin- $\frac{1}{2}$ triangle chain model reduces to the F-AF delta-chain with the basal spins $s_2 = 1$ and the apical spins $s_1 = \frac{1}{2}$.

Though the numbers of the ground states for the models with OBC and PBC are different for finite chains, they are the same (with an exponential accuracy) in the thermodynamic limit $n \rightarrow \infty$ and $G(n) \simeq 2^n$. As a result the residual entropy is

$$\mathcal{S} = \frac{\ln G}{N} = \frac{1}{3} \ln 2 \quad (18)$$

We note also that the ground state degeneracy at $J > 0$ is $G(n) \simeq 2^n$ in comparison with $G(n) = 6^n$ at $J = 0$.

The spin- $\frac{1}{2}$ triangle chain at the transition point can be extended to s_1, s_2 -triangle chain in which the apical and the basal spins are s_1 and s_2 correspondingly and the interaction parameter $\alpha = \frac{1}{2\Delta_1} \frac{s_1}{s_2}$. In particular, this parameter is $\alpha = \frac{1}{4}$ for the delta-chain with $s_1 = \frac{1}{2}$, $s_2 = 1$ which corresponds to the limit $J \rightarrow \infty$ of the $s = \frac{1}{2}$ triangle chain. The ground state degeneracy of the s_1, s_2 -triangle chain can be obtained in the same manner as for the case $s_1 = s_2 = \frac{1}{2}$.

It is interesting to consider the influence of the exponentially large ground state manifold on low-temperature thermodynamics of the model in the magnetic field h . The contribution of the degenerate ground states to the partition function Z_{gs} can be calculated analytically and Z_{gs} has a form (we consider the periodic model)

$$Z_{gs} = 2 \sum_{k=0}^{n/2} C_n^k \cosh \left[\left(\frac{3n}{2} - k \right) \frac{h}{T} \right] + 2C_n^{n/2} \sum_{k=n/2}^{3n/2} \cosh \left[\left(\frac{3n}{2} - k \right) \frac{h}{T} \right] \quad (19)$$

We note that Z_{gs} and all thermodynamics depend on an universal variable $x = h/T$. Of course, the contribution of excited states destroys this universality (see below).

The magnetization M and the susceptibility χ are given by

$$M = T \frac{d \ln Z}{dh}, \quad \chi = T \frac{d^2 \ln Z}{dh^2} \quad (20)$$

The analysis of Eqs.(19) and (20) shows that the magnetization and the susceptibility depend on the relation between x and N . It can be shown that M at $x \gg \frac{1}{N}$ has a form

$$M = \frac{3 + e^{-x}}{6 + 6e^{-x}} N \quad (21)$$

As follows from Eq.(21) the magnetization per spin $m = \frac{M}{N}$ at $\frac{h}{T} \rightarrow 0$ tends to $m = \frac{1}{3}$. Therefore, the spin triangle chain model on the transition line is magnetically ordered at zero temperature and the magnetization undergoes a jump from $m = \frac{1}{2}$ in the ferromagnetic phase to $m = \frac{1}{3}$ on the transition line. The magnetization $m(x)$ given by Eq.(21) is shown in Fig.2 together with that obtained by the exact diagonalization (ED) calculations for the temperatures from $T = 10^{-3}$ to $T = 1$. As can be seen from Fig.2 the magnetization m is, in fact, the function of both x and T .

The magnetization M given by Eqs.(19) and (20) at $x \ll \frac{1}{N}$ is

$$M = d_n x, \quad d_n = \frac{2^n \left(n^2 + \frac{n}{4} \right) + C_n^{n/2} \left(\frac{2}{3} n^3 + n^2 + \frac{n}{3} \right)}{2^n + 2n C_n^{n/2}} \quad (22)$$

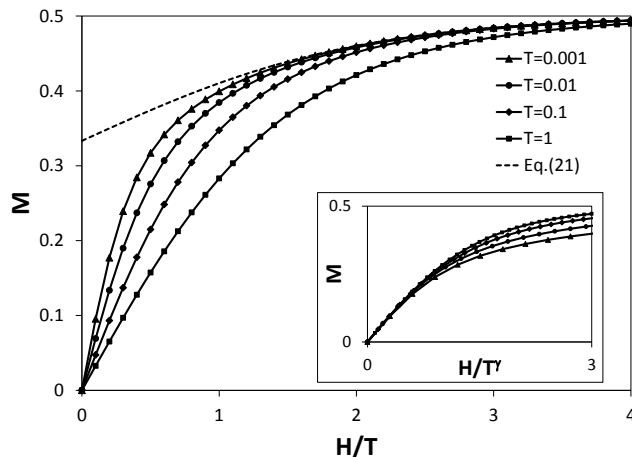


FIG. 2: Magnetization as a function of h/T for isotropic model (1) with $J = 1$ and $n = 6$ at several values of temperature. The inset shows the magnetization vs scaled magnetic field h/T^γ .

and at $N \gg 1$ (but $x \ll \frac{1}{N}$) the magnetization is

$$M = \frac{N^2 x}{27} \quad (23)$$

The uniform magnetic susceptibility χ at $T \rightarrow 0$ can be found from Eq.(22) and it is $\chi = d_n/T$. The quantity $\chi T/N$ at $T \rightarrow 0$ is finite and increases with N as $\chi T/N = 0.823(N = 12)$, $1.1038(N = 18)$, $1.3764(N = 24)$, $1.6436(N = 30)$. For $N \gg 1$, $\chi T/N = N/27$, i.e. it is proportional to N instead of to be a constant. It means that $\chi T/N$ diverges at $T \rightarrow 0$ in the thermodynamic limit and the behavior of χ at large N and small T is described by the finite-size scaling function $\chi = T^{-\gamma} f(NT^{\gamma-1})$ and $\frac{\chi}{N} \sim T^{-\gamma}$ in the thermodynamic limit. Generally, the critical exponent γ depends on Δ_1 and J . We estimate the value of γ for the isotropic model ($\Delta_1 = 1$) and for some values of J using the results of the ED calculations of the magnetization for the chain with $n = 6$ triangles ($N = 18$). An analysis of data on inset in Fig.2 shows that the magnetization at small values of h and T corresponds to the scaling variable $y = h/T^\gamma$ with $\gamma \simeq 1.15$.

We note that the partition function Z_{gs} in Eq.(19) at $h = 0$ does not depend on the temperature and the thermodynamics at $h = 0$ is determined by the contribution of the excited states only. Therefore, it is necessary to study the properties of the spectrum of excitations (with a particular focus on the isotropic case, $\Delta_1 = 1$). One of these points is

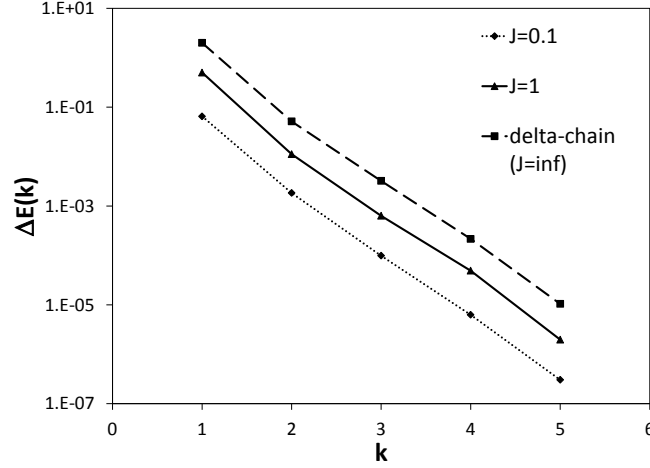


FIG. 3: The gap for k -magnon states, $\Delta E(k)$, for isotropic model (1) with $n = 10$ and $J = 0.1, 1$ and Δ -chain with basal spins $s = 1$, which corresponds to the limit $J \rightarrow \infty$.

related to the value of the lowest excitation in the spin sector $S^z = S_{\max} - k$ (the gap for k -magnon states). The gap ΔE for $k = 1$ can be found from Eq.(6). In particular, for the isotropic model $\Delta E = \frac{2}{3}J$ for $J \ll 1$ and $\Delta E = \frac{1}{2}$ for $J = 1$ and $\Delta E = 2$ for $J \rightarrow \infty$. The gaps decrease rapidly with increasing k as it can be seen from Fig.3 where the gaps for the periodic isotropic chain for $n = 10$ ($N = 30$) are presented for some values of J including the case $J = \infty$. On the base of these results it can be concluded that the gap becomes extremely (exponentially) small for $k \gg 1$. Another important observation that follows from Fig.3 is that the behavior of $\Delta E(k)$ for different values of J are very similar, and coincide with very high accuracy after the corresponding scaling of energy. The latter fact has important consequences that will be discussed below.

A significant characteristic of the spectrum is the distribution of the energy levels (density of states). As an example, we consider this distribution for the isotropic model. At $J = 0$ the spectrum consists of $(n + 1)$ isolated levels with energies $E_0 = 0, E_1 = \frac{3}{2}, E_2 = 3, \dots, E_n = \frac{3n}{2}$. The total number of states is 8^n . The lowest level with $E_0 = 0$ contains 6^n states and the level with $E_k = \frac{3k}{2}$ contains $C_n^k 6^n / 3^k$ states. The neighboring levels are separated from each other by the gap $\Delta E = \frac{3}{2}$. At $J > 0$ each level splits and transforms to the band and a width of the band depends on J . In order to find out the dependence of the spectrum properties on J we

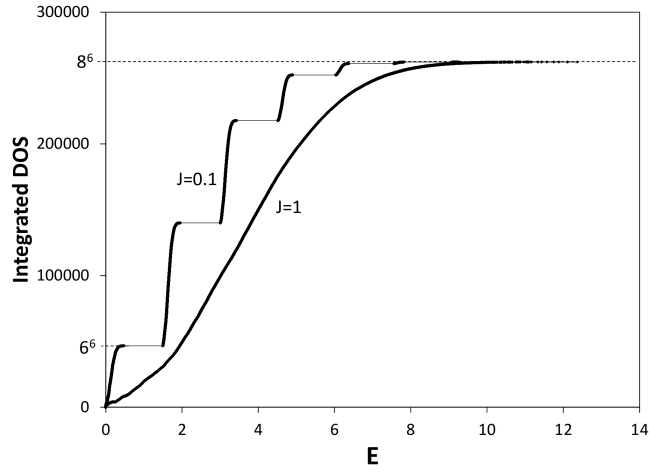


FIG. 4: Integrated density of states of the isotropic model (1) for $J = 0.1; 1$ and $n = 6$.

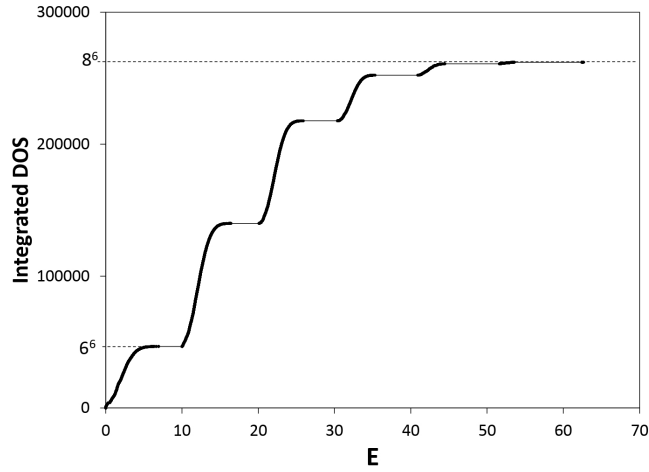


FIG. 5: Integrated density of states of the isotropic model (1) for $J = 10$ and $n = 6$.

calculate the integrated density of states for the isotropic model with $n = 6$ and $J = 0.1; 1; 10$ which are shown in Figs.4,5. As it is seen from these Figures the spectrum for small and large J has a step-like structure with gaps between neighboring bands but the spectrum is gapless for $J = 1$. Our numerical calculations show that the gap ΔE between the lowest band and the next one decreases with increasing J from the value $\Delta E = \frac{3}{2}$ at $J = 0$ to zero

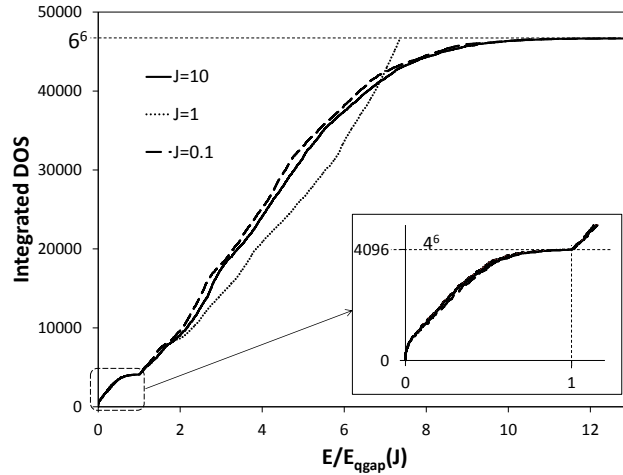


FIG. 6: Low-energy part of the integrated density of states of the isotropic model (1) plotted against the energy normalized by E_{qgap} for $J = 0.1; 1; 10$ and $n = 6$. The inset shows the lowest energy part of the plot.

at $J \simeq 1$. But then ΔE grows again and the gap becomes $\Delta E \simeq J$ for $J \gg 1$. The structure of the lowest band containing 6^6 states is of particular interest because it determines the low-temperature thermodynamics. Corresponding integrated density of states is shown in Fig.6. As it can be seen from Fig.6 in this band there is a low-energy region separated by a quasi-gap (a cusp in the density of states) from the region above the cusp as it is shown in Fig.6 (inset). A notable feature of the spectrum is the fact that the number of states in the low-energy part is 4^6 . We note that a similar spectrum takes place for the model with $n = 4$, where the number of levels below the quasi-gap is 4^4 . Based on these facts, we assume that such specific structure of the spectrum is a general property of the model and the low-energy part consists of 4^n levels below the quasi-gap. This low-energy region also includes $\sim 2^n$ ground states with zero energy.

The position of the quasi-gap depends on J and the results of the calculations of this dependence are shown in Fig.7 for the chain with $n = 6$. At small values of J the quasi-gap energy is $\sim 0.4J$ and it tends to ~ 0.6 for large J . A remarkable feature of the spectrum is that the integrated density of states in the energy region below the cusp is an universal function of the normalized energy $E/E_{qgap}(J)$ for any J as it is shown in Fig.6 (inset).

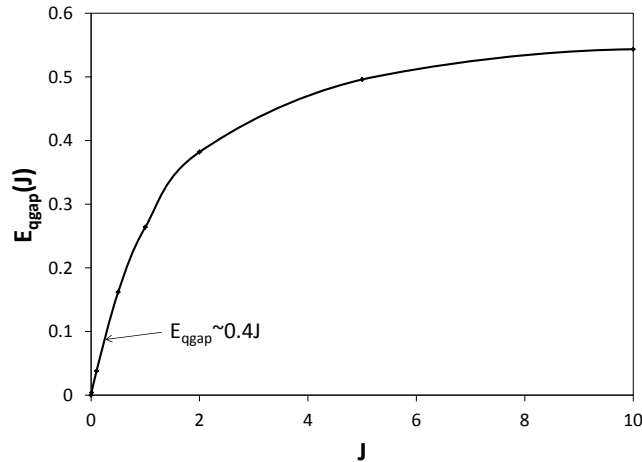


FIG. 7: Dependence of the energy of the 4^n -th level that separates the lowest-energy scale on J for the isotropic model (1).

Similar to this the densities of states in the band of 6^6 states as functions of $E/E_{qgap}(J)$ are very close to each other for small and large J as it is shown in Fig.6. Another remarkable peculiarity of the spectrum is related to a ratio of a width of the lowest band of 6^6 states to the quasi-gap energy $E_{qgap}(J)$. It is almost the same for both small and large J (it is ~ 13) and it is ~ 7 for $J \simeq 1$. We note that these unusual feature of the spectrum as well as the dependence of the quasi-gap energy on J takes place for the model with any n as it follows, for example, from the temperature dependence of the specific heat.

This specific structure of the spectrum determines the low-temperature thermodynamics. In Fig.8 we represent the data for the temperature dependence (in logarithmic temperature scale) of the specific heat $C(T)$ obtained by the ED calculation for the isotropic model with $n = 4$ and $n = 6$ for $J = 0.1$. As it can be seen from Fig.8 the data for $n = 4$ and $n = 6$ deviate from each other for $T < 10^{-4}$ but are close for $T > 10^{-3}$. It indicates that the data for $n = 6$ describe the thermodynamic limit at $T > 10^{-3}$.

The specific heat in Fig.9 for $J = 0.1$ is characterized by the existence of two pronounced maxima at $T \simeq 0.03$ and $T \simeq 1$. In addition to these maxima there is a small low-temperature peak at $T \simeq 0.003$. We propose that the left broad maximum at $T = 0.03$ is determined by 6^n states of the lowest band and the right maximum at $T \simeq 1$ is related to

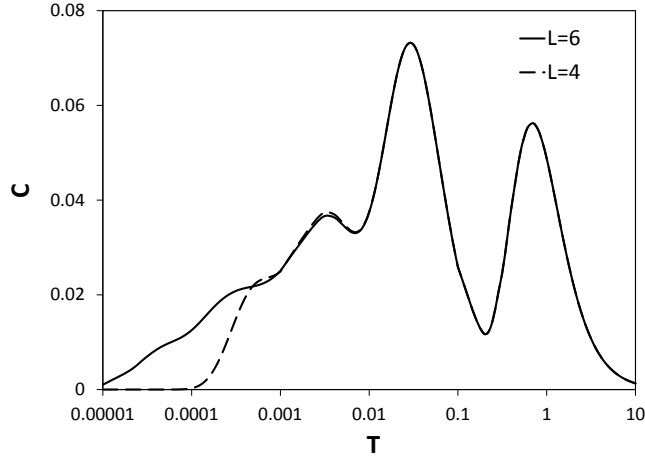


FIG. 8: Dependence of the specific heat on the temperature of the isotropic Hamiltonian (1) with $J = 0.1$ and $n = 4$ (dashed line) and $n = 6$ (solid line).

other high-energy states. Let us denote positions of three maxima as T_1 , T_2 and T_3 from left to right, correspondingly. When J is small, then $T_2 < T_3$. When J increases up to $J \simeq 1$ both broad maxima merge ($T_2 \simeq T_3$) and the spectrum becomes gapless. After that they separate again when J increases. At $J \rightarrow \infty$ both T_1 and T_2 are finite ($T_1, T_2 \simeq 1$) while $T_3 \rightarrow \infty$ as a consequence of removing of the part of high-energy states above the gap to an infinity together with the gap which is $\Delta E \simeq J$. Therefore, in the limit $J \rightarrow \infty$ there are two maxima and $C(T)$ behave as that for the delta-chain. On the other hand, in the limit $J \rightarrow 0$ both T_1 and T_2 tend to zero and $T_3 \simeq 1$. As a result the specific heat for $J = 0$ has one maximum at $T \simeq 1$.

In Fig.10 we represent the temperature dependence of the specific heat for the isotropic model with $n = 6$ and $J = 0.1; 1; 10$. Taking to account an universality of the density of low-energy states as a function of $E/E_{qgap}(J)$ we renormalize the temperature scale as $y = T/E_{qgap}(J)$. Then the results for small and large J are close with each other for different J at $y \leq 1$. To confirm this relation we calculate the contribution of each part of the spectrum to the specific heat. At first, we select the part containing 6^6 states and remove the high-energy states above the gap. The contribution of this part is responsible for the maxima of $C(T)$ at $y \simeq 1$. At second, we select 4^6 low-energy states of the spectrum

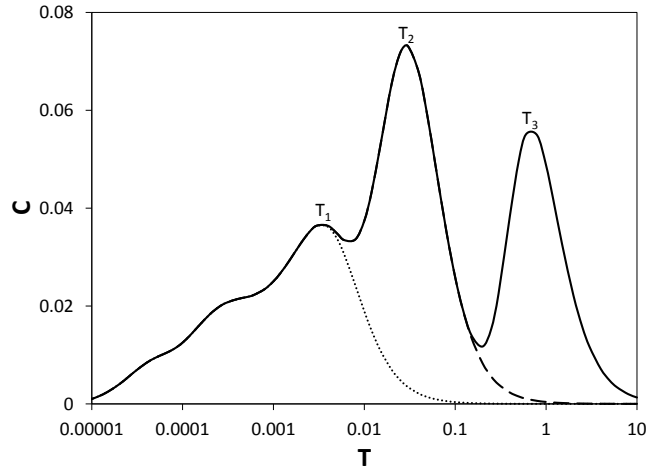


FIG. 9: Dependence of the specific heat on the temperature of the isotropic Hamiltonian (1) with $J = 0.1$ and $n = 6$ (solid line). The specific heat calculated on truncated partition function containing the lowest 4^n (dotted line) and 6^n (dashed line) states.

below the cusp and remove other states. The contributions of these parts are shown in Fig.9 and they reproduce very well corresponding maxima of $C(T)$.

One remark is concerned to the spectrum of model (1) in the limit $J \rightarrow \infty$. In this limit model (1) reduces to the delta-chain with the apical spin $s_1 = \frac{1}{2}$ and the basal spin $s_2 = 1$. The total number states in such model is 6^n in comparison with the number 8^n for the spin triangle chain with finite J . But the spectrum of such delta-chain has one band consisting of two parts and the low-energy region contains 4^n states which is separated by the cusp from the high-energy region, i.e. the structure of the spectrum is the same as for the lowest band of the spin- $\frac{1}{2}$ triangle chain with finite J . The specific heat of such delta-chain has two maxima in accordance with above mentioned transformation of the spectrum at $J \rightarrow \infty$.

A similar temperature dependence of the specific heat is realized for other values of $\Delta_1 < 1$ as is shown in Fig.11 with shoulder instead of the peak at low temperature. The temperature dependence of the entropy per site $s(T)$ demonstrates a stair-step behavior between limits $s_0 = \frac{1}{3} \ln 2$ at $T \rightarrow 0$ and $s = \ln 2$ at $T \rightarrow \infty$.

The $s = \frac{1}{2}$ triangle chain on the transition line between the ferromagnetic and other ground states can be extended to the triangle chain in which the apical and the basal spins

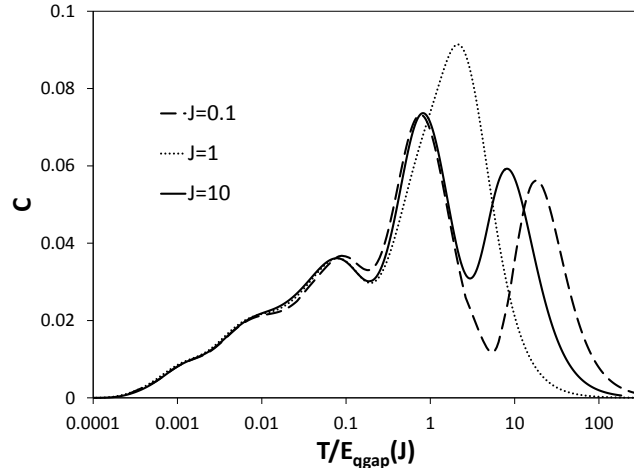


FIG. 10: Dependence of the specific heat on the temperature of the isotropic Hamiltonian (1) with $J = 0.1; 1; 10$ and $n = 6$.

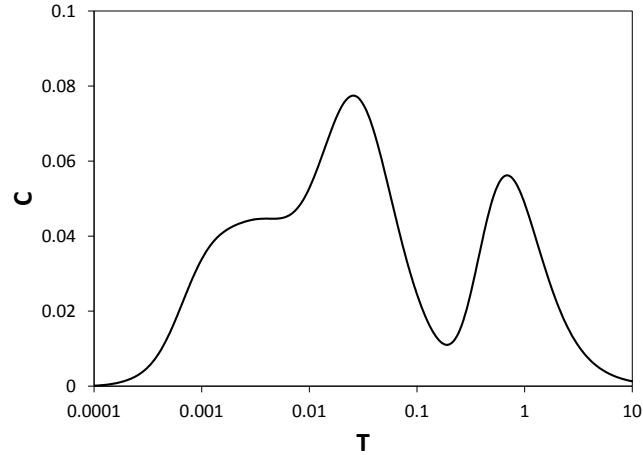


FIG. 11: Dependence of the specific heat on the temperature of the anisotropic Hamiltonian (1) with $\Delta_1 = 0.5$ and $n = 6$.

are s_1 and s_2 , correspondingly. Such model is the one-parametric as well and we can take as this parameter the anisotropy Δ_1 . Then the basal-basal interaction parameters α and Δ_2 are $\alpha = \frac{1}{2\Delta_1} \frac{s_1}{s_2}$ and $\Delta_2 = 2\Delta_1^2 - 1$. The ground state degeneracy of the s_1, s_2 -triangle

chain can be obtained from Eq.(11) with $S_{\max} = (2s_2 + s_1)n$ instead of $\frac{3n}{2}$. The ground state degeneracy does not depend on J . In the limit $J \rightarrow \infty$ spin- s_1, s_2 triangle chain reduces to the delta-chain with the apical spin s_1 and the basal spin $2s_2$. In particular, the $s = \frac{1}{2}$ triangle chain becomes the F-AF delta-chain with $s_1 = \frac{1}{2}, s_2 = 1$ and with the interaction parameter $\alpha = \frac{1}{4\Delta_1}$.

It is interesting to consider the distribution of the energy levels in the spectrum of the spin- s_1, s_2 triangle chain. The total number of states is $(2s_2 + 1)^{2n}(2s_1 + 1)^n$. The distribution has the band structure and the lowest band is separated by the gap $\Delta E \simeq 1$ from the high-energy region. The number of states below the gap is $4^n(s_1 + 2s_2)^n$. The numerical calculations of the integrated density of states for the spin triangle chains for some values of s_1 and s_2 show that the lowest band in the model with the apical spin $s_1 = \frac{1}{2}$ and the basal spin s_2 has low-energy region separated by the cusp from the region above the cusp. The number of states in the region below the cusp is $(4s_2 + 2)^n$ and is the same for any J . This region includes the ground state manifold with zero energy. We note that in the limit $J \rightarrow \infty$ in which the s_1, s_2 -triangle chain reduces to the $s_1, 2s_2$ -delta-chain there is one band in the spectrum with $2^n(4s_2 + 1)^n$ states and there is low-energy region below the cusp and the number of states in this region is $(2s_2 + 2)^n$ as for the triangle chain with finite J . It is interesting to compare the properties of the spectrum of spin- $\frac{1}{2}$ triangle chain with those for the F-AF spin- $\frac{1}{2}$ delta-chain. The spectrum of the latter contains 6^n states and there is a cusp in the density of states. The number of states below the cusp is 3^n . As was shown in [17] such structure of the spectrum leads to the temperature dependence $C(T)$ with two maxima in contrast with that for spin- $\frac{1}{2}$ triangle chain in which $C(T)$ has three peaks.

IV. THE SPIN- $\frac{1}{2}$ TRIANGLE CHAIN WITH STRONG ANISOTROPY OF THE INTERACTIONS

In this Section we consider the spin triangle model in the transition line in the strong anisotropic limit, $\Delta_1 \gg 1$. It is convenient to normalize the Hamiltonian (2) as H_i/Δ_1 and to represent it in a form

$$\begin{aligned} \tilde{H}_i = & -2g \sum_{m=1,2} (s_{i,m}^x s_{i,m+1}^x + s_{i,m}^y s_{i,m+1}^y) - \sum_{m=1,2} (s_{i,m}^z s_{i,m+1}^z - \frac{1}{4}) \\ & + 2g^2 (s_{i,1}^x s_{i,3}^x + s_{i,1}^y s_{i,3}^y) + (1 - 2g^2) (s_{i,1}^z s_{i,3}^z - \frac{1}{4}) \end{aligned} \quad (24)$$

where $g = \frac{1}{2\Delta_1}$.

The Hamiltonian of the model is

$$H = \sum_{i=1}^n \tilde{H}_i + \sum_{i=1}^n V_{i,i+1} \quad (25)$$

At first we consider the limit $g = 0$. At $g = 0$ the model (25) reduces to the Ising triangle model with the Heisenberg ferromagnetic interaction between them. The Ising basal-apical and the basal-basal interactions in each triangle are -1 and $+1$, correspondingly (in the limit $J \rightarrow \infty$ they are -1 and $+\frac{1}{2}$).

Of course, the spectrum of such Ising-Heisenberg Hamiltonian depends on J and in the limit $J \rightarrow \infty$ even the total number of states is 6^n rather than 8^n for $J > 0$. But here we are interested in the low-energy part of the spectrum containing just 6^n states and the numbers of the k -magnon states in this part of the spectrum are the same for any J including the limiting case $J = \infty$.

A most simple way to determine these numbers is just to consider this limiting case. As we note above in the limit $J = \infty$ model (25) for $g = 0$ reduces to the Ising delta-chain with the apical spin $s = \frac{1}{2}$ and the basal spin $\tau = 1$. The Hamiltonian of this Ising model has a form

$$H_{\text{Ising}} = \sum_{i=1}^n [-s_{2i}^z (\tau_{2i-1}^z + \tau_{2i+1}^z - 1) + \frac{1}{2} (\tau_{2i-1}^z \tau_{2i+1}^z - 1) - h (s_{2i}^z + \tau_{2i-1}^z)] \quad (26)$$

where $s_{2i}^z = (\frac{1}{2}, -\frac{1}{2})$, $\tau_{2i-1}^z = (1, 0, -1)$ and h is the magnetic field.

The partition function of the Ising model (26) can be obtained using the transfer-matrix method and the eigenvalues of the transfer matrix satisfy the equation

$$\lambda^3 - \lambda^2(1 + y^2) - \lambda y(1 + y + y^2 + y^3 + y^4) - y^4(1 + y) = 0 \quad (27)$$

where $y = \exp(-\frac{h}{T})$.

The partition function Z_{Ising} is

$$Z_{I \sin g} = \lambda_1^n + \lambda_2^n + \lambda_3^n \quad (28)$$

The ground state energy of (26) is zero and the ground state degeneracy in the spin sector $S^z = (\frac{3n}{2} - k)$ ($0 \leq k \leq 3n$) can be found as coefficients in the expansion of Z_{Ising} in powers of $\exp(-\frac{h}{T})$. The first terms of an expansion of λ on y are

$$\lambda_1 = 1 + y + 2y^3 - y^4 + 3y^5 - 8y^6 + \dots$$

$$\begin{aligned}\lambda_2 &= -y + y^4 - 3y^5 + \dots \\ \lambda_3 &= -y^3 + y^6 + \dots\end{aligned}\quad (29)$$

The number of the ground states of model (26) $W_k(n)$ in the spin sector $S^z = S_{\max} - k$ is

$$W_k(n) = C_n^k + 2(k-2)C_n^{k-2} - (k-3)C_n^{k-3} + 3(k-4)C_n^{k-4} - 8(k-5)C_n^{k-5} + \dots \quad (30)$$

In particular, the number of the ground states in the spin sector $S^z = S_{\max} - k$ with $k \leq 4$ is

$$W_1(n) = n, \quad W_2(n) = C_n^2, \quad W_3(n) = C_n^3 + 2n, \quad W_4(n) = C_n^4 + 4nC_n^2 - n \quad (31)$$

The total number of the ground states of model (26) $G_0(n)$ is given by Eq.(28) with λ_i at $y = 1$. The solutions of Eq.(27) at $y = 1$ are

$$\lambda_1 = \frac{3 + \sqrt{17}}{2}, \quad \lambda_2 = \frac{3 - \sqrt{17}}{2}, \quad \lambda_3 = -1 \quad (32)$$

and $G_0(n)$ is

$$G_0(n) = \lambda_1^n + \lambda_2^n + \lambda_3^n \quad (33)$$

For $n \gg 1$ the total number of the ground states is $G_0(n) = \lambda_1^n = (3.56\dots)^n$.

At $g = 0$ the ground state of the Hamiltonian (25) is $(3.56\dots)^n$ -fold degenerate and at $g \neq 0$ the degeneracy is lifted for each spin sector $S^z = (S_{\max} - k)$ but only partly: some ground states remain degenerate with zero energy and the number of such states is given by Eq.(11). But other states move up. As a result the ground state degeneracy of model (25) at $g \neq 0$ is $G(n) \simeq 2^n$ in contrast with $G_0(n) = (3.56\dots)^n$. At $g \ll 1$ split off levels form a set of low-lying excitations determining the low-temperature thermodynamics.

In the one-magnon sector ($k = 1$) the number of the ground states is $W_1(n) = n$ for both cases $g = 0$ and $g \neq 0$. The same thing takes place in the two-magnon sector where $W_2(n) = C_n^2$ for $g = 0$ and $g \neq 0$. In the three-magnon sector ($k = 3$) there are C_n^3 ground states at $g \neq 0$ and $2n$ states according to Eq.(31) split off from the ground state manifold at $g = 0$ and they are bound magnon complexes. The calculation of these complexes is rather cumbersome and we give a final result for $k = 3$. There are n split off states with the energy $E \sim g^4$ and n states with $E \sim g^2$. The exact diagonalization (ED) calculation of four-magnon complexes show that there are n split off states with $E \sim g^8$, then $n(n-5)$

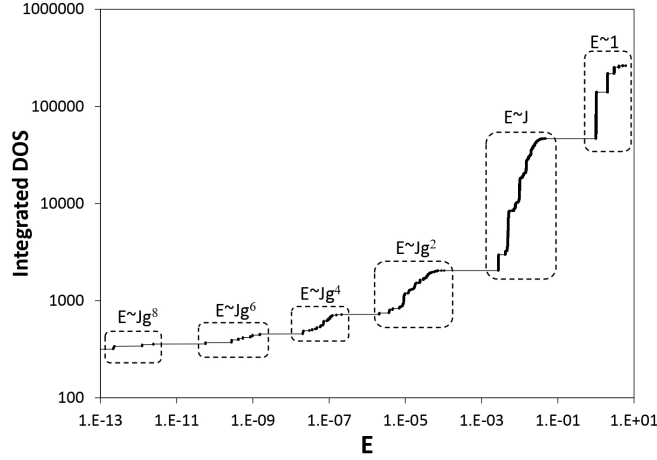


FIG. 12: Integrated density of states of the normalized Hamiltonian (25) with $g = 0.05$, $J = 0.01$ and $n = 6$.

states with $E \sim g^4$ and $n(n+1)$ states with $E \sim g^2$. The total number of split off states is $(4nC_n^2 - n)$ in agreement with the value $W_4(n)$ in Eq.(31).

On a base of the numerical calculations we conclude that the energy of the lowest excitations at $g \ll 1$ in k -magnon sector with $k \geq 3$ is $E \sim g^{4(k-2)}$, then there are excitations with $E \sim g^{4(k-3)}$, $E \sim g^{4(k-4)}$, ... up to $E \sim g^{4(\frac{k}{2}-1)}$, and $E \sim g^{2(k-3)}$, $E \sim g^{2(k-4)}$, ... $E \sim g^2$. Thus, the low-energy excitations in the spin sector with k magnons are divided into parts with the energies from $E \sim g^2$ to $E \sim g^{4(k-2)}$.

The structure of the spectrum and the integrated density of states of model (25) have some features similar to those for the isotropic model. The spectrum has the low- and high-energy regions containing 6^n and $(8^n - 6^n)$ states. The gap ΔE between them decreases from the value $\Delta E = 1 + 2g^2$ at $J = 0$ to zero at $J \simeq 1$. Then ΔE increases and becomes $\Delta E \simeq J$ at $J \gg 1$, i.e. the high-energy part of spectrum goes to infinity at $J \rightarrow \infty$. The width E_w of the low-energy region is changed from $E_w \simeq J$ at small J to $E_w \simeq 1$ at $J \gg 1$. The main difference between the density of states for the cases $\Delta_1 = 1$ and $\Delta_1 \gg 1$ concerns the structure of the region with 6^n states. At $g = 0$ this region corresponds to the low-energy part of the Ising-Heisenberg model and it consists of $G_0(n)$ ground states with zero energy and the part with energies $E \simeq J$ for small J and $E \simeq 1$ for $J \gg 1$. At

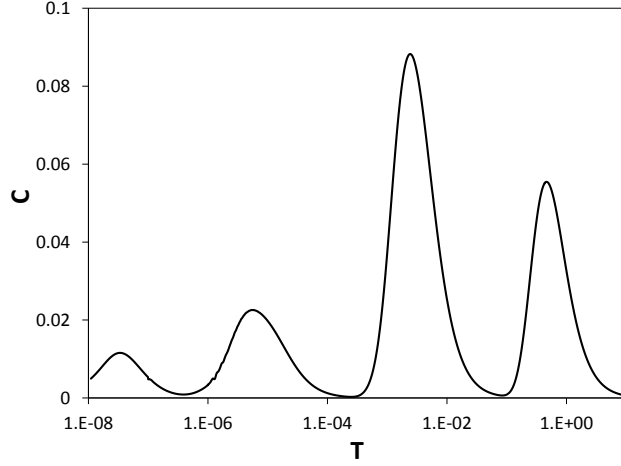


FIG. 13: Dependence of the specific heat on the temperature of the normalized Hamiltonian (25) with $g = 0.05$, $J = 0.01$ and $n = 6$.

$g > 0$, $G_0(n)$ states are split as noted before into the states with $E = 0$, $E \sim g^2$, $E \sim g^4$ and so on as shown on Fig.12 where the integrated density of states of model (25) with $n = 6$ for $g = 0.05$ and $J = 0.01$ is presented. As it can be seen from Fig.12 the low-energy region (up to $E \sim g^2$) is separated by a gap from the region with higher energy. The low-energy region below the gap is divided into the parts with the energies from $E \sim g^2$ to $E \sim g^6$. Such structure of the spectrum leads to the specific features of the low-temperature thermodynamics. The temperature dependence of the specific heat is shown in Fig.13. The low-temperature maxima on the dependence $C(T)$ are related to the corresponding parts of the spectrum with the energies $E \sim g^2$, $E \sim g^4$ and $E \sim g^6$. Two pronounced maxima at $T \simeq J$ and $T \simeq 1$ on Fig.13 are related to the parts of the spectrum with 6^6 and $(8^6 - 6^6)$ states, correspondingly. Similarly to the case $\Delta_1 = 1$ these maxima merge at $J \simeq 1$ and are separated again at $J > 1$. The high-temperature maximum shifts to an infinity at $J \rightarrow \infty$. In the limit $J \rightarrow 0$ the region of the spectrum containing 6^n states has zero energy and the specific heat has one maximum at $T \simeq 1$.

We note that the number of states in the low-energy region below the gap is $G_0(6) = 2042$. It means that this region consists of both the ground states and the energy levels which are split off from the ground state at $g = 0$. We believe that this is a general property of the

strongly anisotropic model (25) and the number of the low-energy states below the gap is $G_0(n)$. We note that this fact takes place for both spin- $\frac{1}{2}$ triangle chain and the delta-chain with spins $s_1 = \frac{1}{2}$, $s_2 = 1$.

However, such property (all state below the gap are split off from the ground state at $g = 0$ and the total number of these states is $(3.56..)^n$ does not valid when g increases. At first, the gap in the spectrum is transformed to the quasi-gap or to the cusp in the density of states as it is in the isotropic model considered above. Secondly, the number of states below the cusp for the isotropic model ($\Delta_1 = 1$) with $n = 6$ is $4^6 = 4096$ rather than 2042. Therefore, the low-energy regions determining the low-temperature thermodynamics are different for the isotropic and the strong anisotropic spin- $\frac{1}{2}$ triangle chain and the number of states in the low-energy region is 4^n for $\Delta_1 = 1$ and $(3.56..)^n$ for $\Delta_1 \gg 1$.

V. SUMMARY

We have studied the ground state and the low-temperature thermodynamics of the frustrated model consisting of the triangles with competing ferro- and antiferromagnetic interactions. The triangles are connected by the ferromagnetic Heisenberg interaction $-J$. At definite conditions between values of the interactions the lowest branch of the one-magnon excitations is dispersionless (flat-band) which leads to the existence of exact ground states which are isolated magnons and specifically overlapping localized multi-magnon complexes. The ground state is macroscopically degenerated in zero magnetic field and the residual entropy is non-zero. Under these conditions the model depends on one parameter and describes the transition line between the ferromagnetic ground state and other ground state phases. The ground state degeneracy does not depend on J but the spectrum of the excitations does. At $J = 0$ the spectrum consists of isolated bands separated by gaps. The lowest part of the spectrum contains 6^n states and is separated from high-energy parts by the gap depending on J . In turns, in this band there is the lowest energy region of 4^n below the quasi-gap (a cusp in the density of states). Therefore, it is possible to divide the spectrum on three parts: high-energy part above the gap, the part below the gap but above the quasi-gap and the low-energy region below the quasi-gap. These three parts are responsible for the peculiarities of the low-temperature thermodynamics of the isotropic model. In particular, these three parts of the spectrum are related to three maxima in $C(T)$ for small and large J . The part

containing 4^n states is related to weak peak in $C(T)$ and other two parts are responsible for broad maxima. At $J \simeq 1$ the gap between them vanishes and two pronounced maxima merge. For $J \gg 1$ the gap is proportional to J and the temperature of the third maximum grows as J . As a result in the limit $J \rightarrow \infty$ two maxima exist as for the F-AF delta chain to which reduces the spin- $\frac{1}{2}$ triangle chain. At $J = 0$ model consist of independent triangles and there is one maximum in $C(T)$ at $T \simeq 1$.

In the limit of strong anisotropic interactions the spectrum has a multi-scale structure which consists of subsets rank-ordered on small parameter. Each subset is responsible for the appearance of the peak in the temperature dependence of the specific heat.

We expect that similar properties of spin- $\frac{1}{2}$ triangle chain can be present in other frustrated spin models, for example, in linear chain of triangular F-AF plaquette with the ferromagnetic Heisenberg interaction between them (kagome-like chain).

Acknowledgments

The numerical calculations were carried out with use of the ALPS libraries [22].

-
- [1] H. T. Diep (ed) 2013 Frustrated Spin Systems (Singapore; World Scientific).
 - [2] C. Lacroix, P. Mendels and F. Mila, eds., Introduction to frustrated magnetism. Materials, Experiments, Theory(Springer-Verlag, Berlin, 2011).
 - [3] O. Derzhko, J. Richter, M. Maksymenko, Int. J. Mod. Phys B **29**, 153007 (2015).
 - [4] M. Maksymenko, A. Honecker, R. Moessner, J. Richter, and O. Derzhko, Phys. Rev. Lett. **109**, 096404 (2012).
 - [5] J. Richter, O. Derzhko and J. Schulenburg, Phys. Rev. Lett. **93**, 107206 (2004).
 - [6] M. E. Zhitomirsky, H. Tsunetsugu, Phys. Rev. B **70**, 100403(R) (2004).
 - [7] O. Derzhko and J. Richter, Phys. Rev. B **70**, 104415 (2004).
 - [8] M. E. Zhitomirsky and H. Tsunetsugu, Phys. Rev. B **75**, 224416 (2007).
 - [9] J. Schnack, H.-J. Schmidt, J. Richter and J. Schulenberg, Eur. Phys. J. B **24**, 475 (2001).
 - [10] J. Richter, J. Schulenburg, A. Honecker, J. Schnack, and H.J. Schmidt, J. Phys.: Condens. Matter **16**, S779 (2004).

- [11] M.E. Zhitomirsky and H. Tsunetsugu, *Progr. Theor. Phys. Suppl.* **160**, 361 (2005).
- [12] S. Capponi, O. Derzhko, A. Honecker, A.M. Lauchli, J. Richter, *Phys. Rev. B* **88**, 144416 (2013).
- [13] J. Richter, O. Krupnitska, V. Balika, T. Krokhmalski, O. Derzhko, *Phys. Rev. B* **97**, 024405 (2018).
- [14] O. Derzhko, J. Richter, *Eur. Phys. J. B* **52**, 23 (2006).
- [15] J. Richter, O. Derzhko, A. Honecker, *Int. J. Mod. Phys B* **22**, 4418 (2008).
- [16] A. Metavitsiadis, C. Psaroudaki, W. Brenig, *Phys. Rev. B* **101**, 235143 (2020).
- [17] V. Ya. Krivnov, D. V. Dmitriev, S. Nishimoto, S.-L. Drechsler, and J. Richter, *Phys. Rev. B* **90**, 014441 (2014).
- [18] D. V. Dmitriev, V. Ya. Krivnov, *Phys. Rev. B* **92**, 184422 (2015).
- [19] D. V. Dmitriev, V. Ya. Krivnov, *J. Phys.: Condens. Matter* **28**, 506002 (2016).
- [20] D. V. Dmitriev, V. Ya. Krivnov, J. Richter, J. Schnack, *Phys. Rev. B* **99**, 094410 (2019); *Phys. Rev. B* **101**, 054427 (2020).
- [21] O. Derzhko, J. Schnack, D. V. Dmitriev, V. Ya. Krivnov, J. Richter, *Eur. Phys. J. B* **93**, 161 (2020).
- [22] F. Alet et al., *J.Phys.Soc.Jpn.Suppl.* **74**, 30 (2005).